PROCEEDINGS OF SCIENCE

Higher QCD corrections for inclusive semileptonic B decays

Matteo Fael[a,*]

[a] *Institut für Theoretische Teilchenphysik*
Karlsruhe Institute of Technology (KIT), 76128 Karlsruhe, Germany

E-mail: matteo.fael@kit.edu

In these proceedings we review the calculation of the total decay rate for inclusive $B \to X_c \ell \bar{\nu}_\ell$ decays to higher orders in perturbative QCD. The partonic rate is obtained via an asymptotic expansion around the limit $1 - m_c/m_b \ll 1$. The same method can be used to compute kinematic moments in case no experimental cuts are applied, i.e. moments of the differential rate integrated over the whole phase space. We discuss the impact of the $O(\alpha_s^3)$ corrections on the total semileptonic decay rate and the moments of the dilepton invariant mass q^2.

Loops and Legs in Quantum Field Theory - LL2022,
25-30 April, 2022
Ettal, Germany

*Speaker

PoS(LL2022)017

1. Introduction

The inclusive semileptonic $B \to X_c \ell \bar{\nu}_\ell$ decay, mediated by the charged-current transition $b \to c\ell\bar{\nu}_\ell$, is a standard probe of the CKM matrix element $|V_{cb}|$. The comparison between the experimental value of the branching ratio $\mathcal{B}(B \to X_c \ell \bar{\nu}_\ell)$ and its theoretical prediction obtained within the framework of the Heavy Quark Expansion allowed the extraction of $|V_{cb}|$ with a 1.2−1.5% accuracy [1, 2]. One of the main result of HQE is that the B meson decay is the same as a free bottom quark decay in the $m_b \to \infty$ limit. In addition higher-order perturbative and non-perturbative corrections can be included in a systematic way as higher α_s and Λ_{QCD}/m_b corrections. Schematically, the total semileptonic decay rate Γ_{sl} has the following structure:

$$\Gamma_{\text{sl}} = \frac{G_F^2 m_b^5}{192\pi^3} A_{\text{EW}} \Bigg\{ \left(1 - \frac{\mu_\pi^2}{2m_b^2}\right) \left(X_0(\rho) + \frac{\alpha_s}{\pi} X_1(\rho) + \left(\frac{\alpha_s}{\pi}\right)^2 X_2(\rho) + \left(\frac{\alpha_s}{\pi}\right)^3 X_3(\rho) \right) + \left(\frac{\mu_G^2}{2m_b^2} - \frac{\rho_{LS}^3}{2m_b^3} \right) \left(Y_0(\rho) + \frac{\alpha_s}{\pi} Y_1(\rho) \right) + \frac{\rho_D^3}{2m_b^3} \left(Z_0(\rho) + \frac{\alpha_s}{\pi} Z_1(\rho) \right) + O\left(\frac{1}{m_b^4}\right) \Bigg\}, \tag{1}$$

where $\alpha_s \equiv \alpha_s^{(4)}(\mu_s)$ is the strong coupling constant at the scale μ_s with 4 active quark flavours, m_b is the bottom quark mass and $\rho = m_c/m_b$ is the ratio between the charm and the bottom quark masses.

The parameters $\mu_\pi^2, \mu_G^2, \rho_D^3$ and ρ_{LS}^3 are non-perturbative matrix elements of local operators between B-meson states. Their values is extracted via global fits of moments of the electron energy spectrum and hadronic invariant mass spectrum [1]. Recently they have been also extracted from moments of the lepton invariant mass q^2 [2], which depend on a reduced set of non-perturbative parameters [3]. The most recent determinations of $|V_{cb}|$ from global fits of inclusive B decays in the kinetic scheme [4] are

$$|V_{cb}| = 42.16\,(51) \times 10^{-3} \text{ [1]}, \qquad |V_{cb}| = 41.69\,(63) \times 10^{-3} \text{ [2]}. \tag{2}$$

In addition, a recent (non-fit) analysis using the 1S scheme found a value consistent with the above determinations, but exhibits a slightly larger uncertainty [5]. The recent improvements in precision of the inclusive $|V_{cb}|$, compared to previous determinations [6, 7], have been achieved thanks to new calculations of the third order correction to the partonic $b \to X_c \ell \bar{\nu}_\ell$ decay rate [8], partially checked in [9], and the $O(\alpha_s)$ corrections to the Wilson coefficient of ρ_D [10, 11]. Perturbative uncertainties constitute one of the limiting factors in the extraction of V_{cb}.

The second improvement comes from the calculation up to $O(\alpha_s^3)$ of the relation between the pole (or $\overline{\text{MS}}$) mass and the kinetic mass [4] of a heavy quark [12, 13]. On the one hand, the scheme conversion is necessary to express the decay rate in terms of a short mass scheme also at $O(\alpha_s^3)$. On the other, the improved relation allowed a more precise conversion of the bottom $\overline{\text{MS}}$ mass, extracted in lattice QCD or sum rules, into the kinetic scheme with a conversion uncertainty of 15 MeV, about a 50% improvement compared to the previous two-loop conversion [14, 15].

In these proceedings we review the calculation of the N^{3}LO corrections to the partonic $b \to X_c \ell \bar{\nu}_\ell$ decay rate. Finite charm mass effects are taken into account via an asymptotic expansion of Feynman integrals in the limit $m_c \simeq m_b$, i.e. $1 - m_c/m_b \ll 1$. The method has been extended also to study higher order corrections to the kinematic moments when no experimental cuts are applied [16].

2. Asymptotic expansion: a two-loop example

The Feynman diagrams contributing to $b \to X_c \ell \bar{\nu}_\ell$ decay depend on two mass scales, m_b and m_c. We obtain finite charm mass effects by performing an asymptotic expansion in the limit $1 - m_c/m_b \ll 1$. It has been shown already at NNLO that the expansion converges quite fast for the physical values of the quark masses [17]. The limit corresponds to a threshold expansion with one heavy mass in the threshold. Let us explain it by considering, as an explicit example, the LO decay rate. The leading order prediction for the decay rate is

$$\Gamma_{\rm sl} = \frac{G_F^2 m_b^5}{192\pi^3} |V_{cb}|^2 \Big(1 - 8\rho^2 - 12\rho^4 \log(\rho^2) + 8\rho^6 - \rho^8\Big). \tag{3}$$

It can be obtained using the optical theorem from the discontinuity of the two-loop diagram shown in Fig. 1, where the external bottom quark momentum is p and there is only one kind of massive internal line (the charm quark) with a mass $m_c \simeq m_b$. Let us assume that the square of the external momentum p^2 and the position of the threshold m_c^2 are close to each other, i.e. $1 - m_c^2/m_b^2 \ll 1$, and expand the Feynman integrals in this limit. The calculation of the two-loop diagram leads to integrals of the form

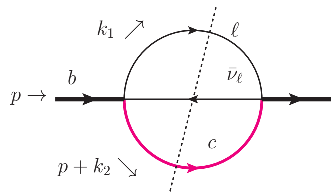

Figure 1: LO contribution to the $b \to X_c \ell \nu$ decay rate. Thick black and magenta lines correspond to bottom and charm quarks, respectively. Thin lines denote the (massless) lepton and antineutrino.

$$I = \int \frac{d^d k_1}{(2\pi)^d} \int \frac{d^d k_2}{(2\pi)^d} \frac{1}{[-k_1^2][-(k_1 - k_2)^2][-(p + k_2)^2 + \rho^2]}. \tag{4}$$

For simplicity we set $p^2 = m_b^2 = 1$, $\rho = m_c/m_b$ and we define $y \equiv 1 - m_c^2/m_b^2$. We apply the expansion by regions [18, 19] and assign to each loop momentum k_1 and k_2 two possible scalings: *hard* (h) when $k \sim m_b$ and *ultrasoft* (u) when $k \sim y \cdot m_b$. The third denominator in (4) comes from the charm propagator. There are only two non-vanishing regions: (hh) and (uu). In all other cases one obtain massless tadpoles which vanish in dimensional regularization.

In the double-hard region, with both momenta k_1 and k_2 hard, the denominator containing the charm mass can be expanded expanded in the following way:

$$\frac{1}{(p + k_2)^2 - \rho^2} = \frac{1}{k_2^2 + 2p \cdot k_2 + y} \overset{\rm (h)}{=} \frac{1}{k_2^2 + 2p \cdot k_2} \sum_{n \geq 0} \left(\frac{-y}{k_2^2 + 2p \cdot k_2} \right)^n. \tag{5}$$

Such expansion leads to two-loop on-shell integrals of the form

$$\begin{aligned} I_{\rm hh} &= \int \frac{d^d k_1}{(2\pi)^d} \int \frac{d^d k_2}{(2\pi)^d} \frac{1}{[-k_1^2][-(k_1 - k_2)^2]} \sum_{n \geq 0} \frac{(-y)^n}{[-k_2^2 - 2p \cdot k_2]^{n+1}} \\ &= \left(\frac{i}{(4\pi)^{2-\epsilon}} \right)^2 \sum_{n \geq 0} (p^2)^{1-n-2\epsilon} (-y)^n \frac{\Gamma(1-\epsilon)^2 \Gamma(\epsilon) \Gamma(-n - 4\epsilon + 3) \Gamma(n + 2\epsilon - 1)}{\Gamma(n+1) \Gamma(2 - 2\epsilon) \Gamma(-n - 3\epsilon + 3)}, \end{aligned} \tag{6}$$

where $\epsilon = (4 - d)/2$. The contribution from the hard region contains no imaginary part and therefore can be always neglected, since we are interested only in the discontinuity.

In case the loop momentum k_2 scales as ultrasoft, the massive propagator is expanded as

$$\frac{1}{(p+k_2)^2-\rho^2} = \frac{1}{k_2^2+2p\cdot k_2+y} \stackrel{\text{(u)}}{=} \frac{1}{2p\cdot k_2+y}\sum_{n\geq 0}\left(\frac{-k_2^2}{2p\cdot k_2+y}\right)^n . \qquad (7)$$

Note that the ultrasoft region yields the well know heavy-quark propagator in HQET. The parameter y is often called in this contest the *residual mass* [20]. In an HQET framework, such residual mass would arise by considering the QCD Lagrangian with two heavy quarks, bottom and charm, and by taking the $m_c, m_b \to \infty$ limit applying a rephasing of the charm and bottom field with the same mass parameter m_b. The contribution to (4) from the double ultrasoft region is

$$\begin{aligned} I_{\text{uu}} &= \int \frac{d^d k_1}{(2\pi)^d}\int \frac{d^d k_2}{(2\pi)^d}\frac{1}{[-k_1^2][-(k_1-k_2)^2]}\sum_{n\geq 0}\frac{(k_2)^n}{[-2p\cdot k_2-y]^{n+1}} \\ &= \left(\frac{i}{(4\pi)^{2-\epsilon}}\right)^2\sum_{n\geq 0}(p^2)^{2\epsilon-n-2}(-y)^{n-4\epsilon+3}\frac{\Gamma(1-\epsilon)\Gamma(n-\epsilon+1)\Gamma(-n+4\epsilon-3)}{\Gamma(1-n)\Gamma(n+1)} . \end{aligned} \qquad (8)$$

From the re-expansion of the factor $(-y)^{-4\epsilon}$ in the limit $\epsilon \to 0$ we generate $\log(-y) = \log(y) + i\pi$ which yields the desired imaginary part. E.g. for $n = 0$ we have

$$I_{uu} = \left(\frac{ie^{-\epsilon\gamma_E}}{(4\pi)^{2-\epsilon}}\right)^2 y^3\left[+\frac{1}{24\epsilon}+\frac{11}{36}-\frac{\log(-y)}{6}+O(\epsilon)\right]+O(y^4). \qquad (9)$$

The final prediction for the LO decay rate can be written as

$$\Gamma_{\text{sl}} = \frac{G_F^2 m_b^5}{192\pi^3}|V_{cb}|^2\sum_{n=5}^{\infty}\frac{24}{n(n-1)(n-2)}y^n . \qquad (10)$$

To improve the convergence of the series, it is convenient to rewrite the expansion in the parameter $\delta = 1 - m_c/m_b$ with $y = 2\delta - \delta^2$. We obtain

$$\Gamma_{\text{sl}} = \frac{G_F^2 m_b^5}{192\pi^3}|V_{cb}|^2\left[\frac{64}{5}\delta^5-\frac{96}{5}\delta^6+\frac{288}{35}\delta^7+\sum_{n=8}^{\infty}\frac{576}{(n-4)(n-3)(n-2)(n-1)n}\delta^n\right] . \qquad (11)$$

With the parameter δ the coefficients in the series are suppressed by $1/n^5$ for large n, while using y the coefficients are suppressed only by $1/n^3$. This fact suggests to employ δ as expansion parameter also at higher orders in α_s, even if y is the natural expansion parameter arising from the Feynman diagrams since odd power of m_c do not appear in the calculation.

3. Details of the calculation to second and third order

The asymptotic expansion described in the previous section can be applied also to higher orders in QED. With the help of the optical theorem we can express the $b \to X_c \ell \nu$ matrix element integrated over the whole phase space in terms of the discontinuity of $b \to b$ forward scattering amplitudes like in Fig. 1. To calculate corrections up to $O(\alpha_s^3)$ we have to add up to three more loops, i.e. we must consider five-loop diagrams.

It is also possible to consider moments of the differential rate when no restriction is applied on the final state particles. For instance, the moments of the leptonic invariant mass q^2, defined by

$$Q_n \equiv \int (q^2)^n \frac{d\Gamma_{\rm sl}}{dq^2}\, \mathrm{d}q^2, \tag{12}$$

are obtained by simply multiplying the integrand of forward scattering amplitude by $(q^2)^n$ and proceeding with the calculation as in the case of the decay rate.

The structure of the Feynman diagrams allows the direct integration of the massless neutrino-lepton loop which leads to an effective propagator raised to an ϵ-dependent power. At this point we apply the expansion by region, and consider all loop momenta to scale either hard or ultrasoft. The all-hard region can be ignored since it contains no imaginary part. The loop integration w.r.t. the dilepton momenta q can be performed analytically without applying integration-by-part (IBP) relations. In fact the momentum q must always be ultrasoft. Integrals depending on loop momenta other the q which scale as hard naturally factorize out. The crucial observation is that also in case another loop momentum is ultrasoft, one can factorize out the integration w.r.t. q by exploiting the linear dependence of the ultrasoft propagators on the loop momenta (for more details see [13]). Therefore, we are able to analytically carry out the integration w.r.t. q without the need of an IBP reduction and we remain at most with three-loop integrals that need to be reduced to master integrals.

After asymptotic expansion of the Feynman diagrams, we find linearly dependent propagators. This requires a partial fraction decomposition in order to define integral families for the IBP reduction. We employ the program LIMIT [21] to automate the partial fraction decomposition in case of linearly dependent denominators. The master integrals for the ultrasoft regions were computed up to three loops in [12, 13]. All triple-hard master integrals can be found in Ref. [22].

For the total rate and kinematic moments, we have computed the first 16, 11 and 8 expansion terms in δ at order $\alpha_s, \alpha_s^2, \alpha_s^3$, respectively. For the total rate this corresponds to an expansion up to δ^{12} since the leading term starts at δ^5. Such deep expansion is necessary to obtain accurate predictions, especially for the central moments. Feynman propagators must be expanded up to 8th or 10th order, leading to intermediate expressions of the order of several hundred GB. They must be handled by `FORM` [24] in an optimized way in order to avoid an uncontrolled grow of the number of terms. Furthermore, for some of the integral families, individual propagators are raised to positive and negative powers up to 12, which constitutes a non-trivial task for the IBP reduction, and we had to rely on a private version of the program `FIRE` [25].

4. Results at N^{3}LO

Our main results are the analytic expressions for the corrections up to $O(\alpha_s^3)$ to the total rate, corresponding to the functions $X_{1,2,3}(\rho)$ in Eq. (1), and similarly for the kinematic moments. In the calculation we renormalized the bottom and charm quark masses in the pole scheme.

In Fig. 2a we show the third order correction to the rate $X_3(\rho)$ as a function of $\rho = 1 - m_c^{\rm pole}/m_b^{\rm pole}$ where the different curves contain different expansion depths in δ. One observes a rapid convergence for values of ρ close to the physical point $\rho \simeq 0.25$. In particular, the curves including terms up to

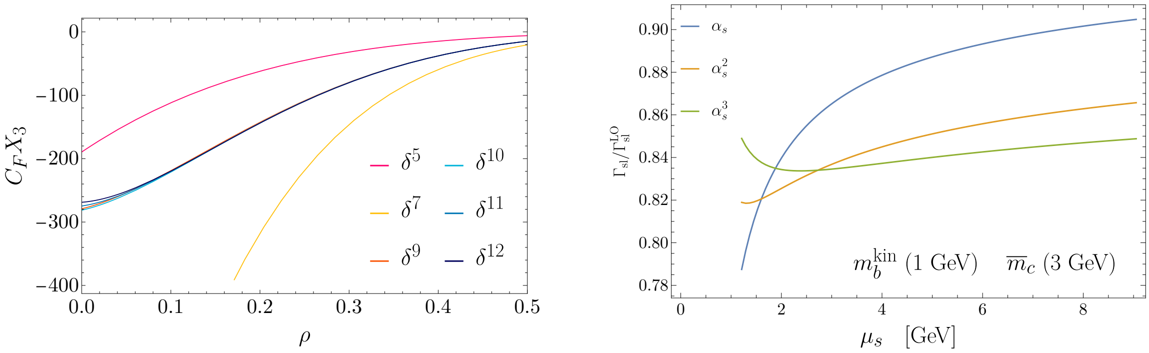

(a) **(b)**

Figure 2: (Left) The $O(\alpha_s^3)$ coefficient to the decay rate (see Eq. (1)) as a function of $\rho = m_c^{\rm pole}/m_b^{\rm plot}$ for different expansion depth in δ. (Right) The partonic decay rate as a function of the renormalization scale μ_s.

$\delta^{10,11,12}$ cannot be distinguished in the plot. We estimate $X_3(\rho = 0.28) = -68.4 \pm 0.3$, where the uncertainty is obtained multiplying the δ^{12} term by a factor of five.

For phenomenological predictions one needs to express the quark masses in a short distance scheme. We adopt the kinetic scheme for the bottom quark mass and the $\overline{\rm MS}$ mass for the charm quark. We also consider the $1S$ scheme [23] for the bottom. In this case we express the charm quark mass via the Heavy Quark Effective Theory (HQET) relation to pole bottom quark mass and (averaged) D and B meson masses. With the input values $m_b^{\rm kin}(1\text{ GeV}) = 4.526$ GeV, $m_b^{1S} = 4.666$ GeV and $\overline{m}_c(3\text{ GeV}) = 0.993$ GeV, we obtain for $\Gamma(b \to X_c \ell \bar{\nu}_\ell)/\Gamma_0$ and $\mu_s = m_b$

$$\begin{aligned} m_b^{\rm kin}, \overline{m}_c(3\text{ GeV}): &\quad 0.700\,(1 - 0.116 - 0.035 - 0.010)\,, \\ m_b^{1S}, m_c^{\rm HQET}: &\quad 0.555\,(1 - 0.095 - 0.030 - 0.011)\,, \end{aligned} \tag{13}$$

where the different α_s orders are displayed separately. One can observe a good behaviour of the perturbative series, with the relative size of the third order correction being about 1%.

In Fig. 2b we show the partonic decay rate as a function of the renormalization scale μ_s of $\alpha_s(\mu_s)$ for the m_b in the kinetic scheme and the m_c in the $\overline{\rm MS}$ scheme. One observes that over the whole range $m_b^{\rm kin}/4 < \mu_s < 2m_b^{\rm kin}$ the dependence on μ_s decreases after including higher order corrections. At NLO the variation is of about 5.6% while at NNLO one still observes a 2.4% variation. The inclusion of the N^{3}LO corrections bring the residual scale uncertainty at the level of 0.8%, so well below the percent level.

Let us discuss now the impact of higher order corrections for kinematic moments, in particular for the q^2 moments. The central moments q_n of the dilepton inveriant mass q^2 are defined via

$$\langle (q^2)^n \rangle \equiv \frac{Q_n}{Q_0}, \qquad q_1 = \langle q^2 \rangle, \qquad q_{n>1} = \left\langle \left(q^2 - \langle q^2 \rangle\right)^n \right\rangle. \tag{14}$$

The analytic calculation of the Feynman diagrams yields the expressions for the moments Q_n in (12) up to third order. To assemble central moments q_n, we start with the expressions for the various Q_n in the pole scheme considering also the power corrections up to $1/m_b^3$ and we convert them to the kinetic scheme. In a second step, the ratios in Eq. (14) are reexpanded up to α_s^3 (to leading order in

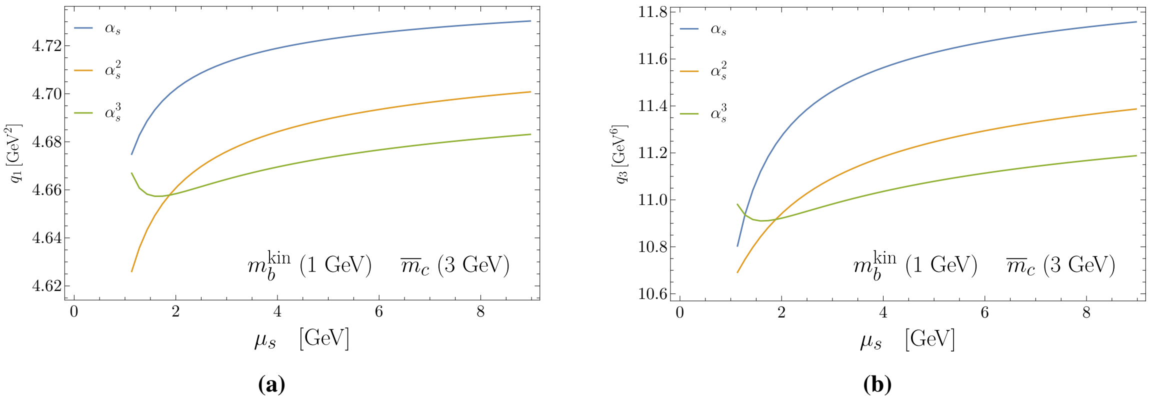

Figure 3: Scale dependence for the first and third central moments of q^2.

$1/m_b$) and up to $O(1/m_b^3)$ for the power corrections. Our results for $\hat{q}_n \equiv q_n/m_b^{2n}$ are

$$\begin{aligned}
\hat{q}_1 &= 0.232947\Big[1 - 0.0106332_{\alpha_s} - 0.007100(16)_{\alpha_s^2} - 0.00326(13)_{\alpha_s^3} - 0.0875(97)_{\rm pw}\Big],\\
\hat{q}_2 &= 0.0235256\Big[1 - 0.0359328_{\alpha_s} - 0.0175591(28)_{\alpha_s^2} - 0.00677(17)_{\alpha_s^3} - 0.237(27)_{\rm pw}\Big],\\
\hat{q}_3 &= 0.00145109\Big[1 - 0.0700256_{\alpha_s} - 0.030529(71)_{\alpha_s^2} - 0.01282(12)_{\alpha_s^3} - 0.726(94)_{\rm pw}\Big],\\
\hat{q}_4 &= 0.0012016\Big[1 - 0.0585099_{\alpha_s} - 0.0342994(88)_{\alpha_s^2} - 0.01597(20)_{\alpha_s^3} - 0.631(77)_{\rm pw}\Big]. \qquad (15)
\end{aligned}$$

For each moment we factorize out the tree-level prediction and show the size of the $\alpha_s, \alpha_s^2, \alpha_s^3$ corrections (denoted by $X_{\alpha_s^n}$). The quoted uncertainties come from the finite number of terms computed in the δ expansion. We denote the sum of all $1/m_b^2$ and $1/m_b^3$ corrections by the subscript "pw". Its uncertainty is based on the parametric uncertainties on the HQE parameters from the fit of Ref. [1]. We observe a good behaviour of the perturbative series, with coefficients precisely determined via the asymptotic expansion in δ.

The size of the $O(\alpha_s^2)$ corrections are of few percent while third order corrections are about a factor of two smaller and in the range of 0.5 - 2%. Higher power corrections are sizable and as large as 70% of the leading order contribution for q_3 and q_4. In Fig. 3 we show the dependence of q_1 and q_3 on the renormalization scale μ_s. For q_1 dependence on μ_s decreases most notably only after inclusion of the third order corrections, from a 3.7% variation at NNLO to a 2.5% at N^{3}LO. Also for q_3 the scale variation is of 1.7%, 1.6% at NLO and NNLO, while it reduces to 1% at N^{3}LO.

5. Conclusions

We reviewed the calculation of the third order QCD corrections for the decay rate of $b \to X_c \ell \bar{\nu}_\ell$ and its kinematic moments (without cuts). The results are obtained by performing an asymptotic expansion in $\delta = 1 - m_c/m_b$. Even if the parameter is rather large for physical values of m_c and m_b ($\delta \simeq 0.7$), the series provides an excellent approximation for phenomenological studies. The size of the $O(\alpha_s^3)$ corrections are of the order of 1% when considering a short mass scheme for the bottom quark mass, e.g. kinetic or 1S mass. Similar behaviours are observed for the q^2 central moments, with residual scale dependence ranging between 2% and 1% depending on the order of the moment.

Acknowledgements

I thank K. Schönwald and M. Steinhauser for the nice and fruitful collaboration. I also thank P. Gambino for comments and suggestions about Ref. [16]. This research was supported by the Deutsche Forschungsgemeinschaft (DFG, German ResearchFoundation) under grant 396021762 – TRR 257 "Particle Physics Phenomenology after the Higgs Discovery".

References

[1] M. Bordone, B. Capdevila and P. Gambino, Phys. Lett. B **822** (2021), 136679 [arXiv:2107.00604 [hep-ph]].

[2] F. Bernlochner, M. Fael, K. Olschewsky, E. Persson, R. van Tonder, K. K. Vos and M. Welsch, [arXiv:2205.10274 [hep-ph]].

[3] M. Fael, T. Mannel and K. Keri Vos, JHEP **02** (2019), 177 [arXiv:1812.07472 [hep-ph]].

[4] I. I. Y. Bigi, M. A. Shifman, N. Uraltsev and A. I. Vainshtein, Phys. Rev. D **56** (1997), 4017-4030 [arXiv:hep-ph/9704245 [hep-ph]].

[5] Y. Hayashi, Y. Sumino and H. Takaura, Phys. Lett. B **829** (2022), 137068 [arXiv:2202.01434 [hep-ph]].

[6] P. Gambino and C. Schwanda, Phys. Rev. D **89** (2014) no.1, 014022 [arXiv:1307.4551 [hep-ph]].

[7] A. Alberti, P. Gambino, K. J. Healey and S. Nandi, Phys. Rev. Lett. **114** (2015) no.6, 061802 [arXiv:1411.6560 [hep-ph]].

[8] M. Fael, K. Schönwald and M. Steinhauser, Phys. Rev. D **104** (2021) no.1, 016003 [arXiv:2011.13654 [hep-ph]].

[9] M. Czakon, A. Czarnecki and M. Dowling, Phys. Rev. D **103** (2021), L111301 [arXiv:2104.05804 [hep-ph]].

[10] T. Mannel and A. A. Pivovarov, Phys. Rev. D **100** (2019) no.9, 093001 [arXiv:1907.09187 [hep-ph]].

[11] T. Mannel, D. Moreno and A. A. Pivovarov, Phys. Rev. D **105** (2022) no.5, 054033 [arXiv:2112.03875 [hep-ph]].

[12] M. Fael, K. Schönwald and M. Steinhauser, Phys. Rev. Lett. **125** (2020) no.5, 052003 [arXiv:2005.06487 [hep-ph]].

[13] M. Fael, K. Schönwald and M. Steinhauser, Phys. Rev. D **103** (2021) no.1, 014005 [arXiv:2011.11655 [hep-ph]].

[14] A. Czarnecki, K. Melnikov and N. Uraltsev, Phys. Rev. Lett. **80** (1998), 3189-3192 [arXiv:hep-ph/9708372 [hep-ph]].

[15] P. Gambino, JHEP **09** (2011), 055 [arXiv:1107.3100 [hep-ph]].

[16] M. Fael, K. Schönwald and M. Steinhauser, JHEP **08** (2022), 039 [arXiv:2205.03410 [hep-ph]].

[17] M. Dowling, J. H. Piclum and A. Czarnecki, Phys. Rev. D **78** (2008), 074024 [arXiv:0810.0543 [hep-ph]].

PoS(LL2022)017

[18] M. Beneke and V. A. Smirnov, Nucl. Phys. B **522** (1998), 321-344 [arXiv:hep-ph/9711391 [hep-ph]].

[19] V. A. Smirnov, Springer Tracts Mod. Phys. **250** (2012), 1-296

[20] A. F. Falk, M. Neubert and M. E. Luke, Nucl. Phys. B **388** (1992), 363-375 [arXiv:hep-ph/9204229 [hep-ph]].

[21] F. Herren, "Precision Calculations for Higgs Boson Physics at the LHC - Four-Loop Corrections to Gluon-Fusion Processes and Higgs Boson Pair-Production at NNLO,", Ph.D. thesis, KIT, Karlsruhe.

[22] R. N. Lee and V. A. Smirnov, JHEP **02** (2011), 102 [arXiv:1010.1334 [hep-ph]].

[23] A. H. Hoang, Z. Ligeti and A. V. Manohar, Phys. Rev. D **59** (1999), 074017 [arXiv:hep-ph/9811239 [hep-ph]].

[24] B. Ruijl, T. Ueda and J. Vermaseren, [arXiv:1707.06453 [hep-ph]].

[25] A. V. Smirnov and F. S. Chuharev, Comput. Phys. Commun. **247** (2020), 106877 [arXiv:1901.07808 [hep-ph]].

PoS(LL2022)017